analytical chemistry

Subscriber access provided by Stockholm University Library

Article

Charge Transfer Platform and Catalytic Amplification of Phenanthroimidazole Derivative: A New Strategy for DNA Bases Recognition

Nannan Lu, He Liu, Rui Huang, Yue Gu, Xiaoyi Yan, Tingting Zhang,
Zhiqian Xu, Haixin Xu, Yue Xing, Yu Song, Xuwen Li, and Zhiquan Zhang

Anal. Chem., **Just Accepted Manuscript** • DOI: 10.1021/acs.analchem.9b02746 • Publication Date (Web): 20 Aug 2019

Downloaded from pubs.acs.org on August 22, 2019

Just Accepted

“Just Accepted” manuscripts have been peer-reviewed and accepted for publication. They are posted online prior to technical editing, formatting for publication and author proofing. The American Chemical Society provides “Just Accepted” as a service to the research community to expedite the dissemination of scientific material as soon as possible after acceptance. “Just Accepted” manuscripts appear in full in PDF format accompanied by an HTML abstract. “Just Accepted” manuscripts have been fully peer reviewed, but should not be considered the official version of record. They are citable by the Digital Object Identifier (DOI®). “Just Accepted” is an optional service offered to authors. Therefore, the “Just Accepted” Web site may not include all articles that will be published in the journal. After a manuscript is technically edited and formatted, it will be removed from the “Just Accepted” Web site and published as an ASAP article. Note that technical editing may introduce minor changes to the manuscript text and/or graphics which could affect content, and all legal disclaimers and ethical guidelines that apply to the journal pertain. ACS cannot be held responsible for errors or consequences arising from the use of information contained in these “Just Accepted” manuscripts.

is published by the American Chemical Society. 1155 Sixteenth Street N.W.,
Washington, DC 20036

Published by American Chemical Society. Copyright © American Chemical Society.
However, no copyright claim is made to original U.S. Government works, or works
produced by employees of any Commonwealth realm Crown government in the course
of their duties.

Charge Transfer Platform and Catalytic Amplification of Phenanthroimidazole Derivative: A New Strategy for DNA Bases Recognition

Nannan Lu[a], He Liu[a], Rui Huang[a], Yue Gu[a], Xiaoyi Yan[a], Tingting Zhang[a], Zhiqian Xu[a], Haixin Xu[a], Yue Xing[a], Yu Song[a], Xuwen Li[a], Zhiquan Zhang[a]*

[a] College of Chemistry, Jilin University, Changchun 130012, China

---

ABSTRACT: Researches about DNA composition have concentrated on DNA damage in the past few decades. However, it still remains a great challenge to construct a rapid, facile and accurate approach for simultaneously monitoring four DNA bases, guanine (G), adenine (A), thymine (T) and cytosine (C). Herein, a novel electrochemical sensor based on phenanthroimidazole derivative, 2-(4-Bromophenyl)-1-phenyl-1H-phenanthro[9,10-d]-imidazole (PPI), is successfully fabricated by a simple electrochemical method. The bromophenyl group in PI could expand their aromatic plane, induce the π-conjugated extension and enhance the charge transfer and π-π interaction. The phenyl group at N1 position could regulate the intermolecular interaction, which could promote the possibility of intermolecular connection. The PPI polymer (poly(PPI)) with π-electron enriched conjugation architecture has been applied in simultaneous determination of G, A, T and C in neutral solution by square wave voltammetry (SWV) method with well-separated peak potentials at 0.714, 1.004, 1.177 and 1.353 V, respectively. The sensor functionalized with poly(PPI) exhibits wide linear response for G, A, T and C in the concentration ranges of 3-300 μM, 1-300 μM, 30-800 μM and 20-750 μM, respectively. With favorable selectivity, stability and reproducibility, the sensor is successfully utilized to monitor four DNA bases in real samples, displaying a promising prospect for electrochemical sensing devices.

The human chromosome, a natural biopolymer with a double-helical structure, is composed of a complicated combination of deoxyribonucleic acid (DNA). As an important biomolecular, the biological function of DNA can be realized via integration of DNA bases: guanine (G), adenine (A), thymine (T) and cytosine (C).[1,2] Therefore, the complete combination of DNA bases in organism is essential to maintain the genetic information and biological function. However, some factors, like lifestyle stress, ultraviolet or infrared radiation exposure and accumulation of carcinogenic chemicals in human body, may lead to the DNA damage by insertions, deletions or translocations of the nucleobases in the sequence of DNA.[3] The unusual changes of bases in organism can result in deficiency or mutation of immune system and may cause various diseases, including cancers, diabetes, epilepsy, Parkinson's and Alzheimer's diseases.[4] Hence, the development of appropriate methods to accurately and sensitively detect DNA bases is very significant in clinical diagnosis and bioanalytical chemistry.

Up to now, various analytical techniques have been proposed for detection of DNA bases, such as high-performance liquid chromatography,[5] mass spectrometry,[6] spectroscopic approaches,[7] chemiluminescence[8] and capillary electrophoresis.[9] As is known, extra separation processes are necessary to detect the bases using above mentioned methods. The time-consuming pretreatment procedures are requested and determination errors are inevitably introduced in the process of detection.[10] Such limitations significantly restrict their further applications. Compared to above methods, electrochemical approaches show many merits of rapid response, high sensitivity, good selectivity and low cost, which make them excellent alternatives to directly determine targets without sample pretreatment processes.[2] Generally, purine bases (G and A) are detectable at bare glassy carbon electrode (GCE). Nevertheless, it is relatively difficult to acquire oxidation signal of pyrimidine bases (T and C) since they request higher oxidation potential and exhibit slower electron transfer kinetics.[11] Therefore, it is necessary to explore new materials for comprehensive analysis DNA bases with a wide oxidation potential window, high electrocatalytic activity and good sensitivity.

In recent years, various materials have been utilized to determine DNA bases, including carbon materials,[12] noble and transition metals,[13,14] transition metal dichalcogenides[3] and conducting polymers.[15] Specifically, conducting polymers have drawn our attention in terms of their π-π conjugated electronic transfer system with rapid electron migration, satisfied electrocatalytic capability for biological molecules and strong affinity to the electrode surface.[16,17] The conducting polymers with π-π conjugated electron can form the "molecular wire".[18] Amplification signal can be acquired with conjugated polymers in molecular wire structure than other small molecular as well as inorganic semiconductor materials, resulting from the outstanding conductivity of the wire-like skeleton structure.[19] Despite that many researches have combined conducting polymers with other materials to construct composites for monitoring DNA bases. The synthesis of composites related with complicated and time-consuming processes and they could only be utilized for individual or simultaneous detection of G and A. [20-23] For example, Yari et al. developed multiwall carbon nanotubes-Fe_3O_4@polydomamine-Ag composite modified electrode to detect G and A. It showed no response toward T and C and the preparation procedure was complicated.[13] Thus, it still remains a great challenge to develop a facile electrochemical analysis assay using conducting polymer materials to simultaneously detect the four DNA bases.

Inspired by the relationship between the structure and property, imidazole derivative has come into our sights. As an important imidazole derivative, phenanthroimidazole (PI), with extended π-conjugation architecture of fused imidazole, endows itself with outstanding charge transporting capabilities. The rigidity of PI could contribute to reducing the reorganization energy in the charge transfer process. Meanwhile, PI unit also possesses high electron affinity, high thermal stability, ease of preparation, adjustable absorption and emission properties.[24] All these features favor it to be a significant building block to design the versatility of materials in many fields, including fluorescent sensors and probes,[25] light-emitting electrochemical cells and organic electrosynthesis.[26] Furthermore, PI heterocyclic ring derivatives not only compose the core of various natural products but also can be employed in designing the bioactive agents in therapy of diseases. There are several evidence to reveal that these compounds have anticancer, antimicrobial and antioxidant activities, which have been used as DNA-structural probe, DNA-photocleavage reagent and anticarcinogenic drugs.[27-29] Because of these characteristics, the functionalized PI derivative may emerge as a novel biological electrocatalyst for electrochemical determination of DNA bases. Nevertheless, the applications of PI compounds in electrochemical sensing fields are seldom reported.

In this work, 2-(4-Bromophenyl)-1-phenyl-1H-phenanthro[9,10-d]-imidazole (PPI) have been designed and utilized to construct a novel electrochemical sensor for simultaneous detection of G, A, T and C for the first time. The introduction of bromophenyl group to PI via C2 position could expand their aromatic plane and induce the π-conjugated extension, resulting in the higher intensity of intramolecular charge transfer and π-π interactions.[30] The phenyl group substituent at N1 position could control the intermolecular interaction,[31] improving the possibility of intermolecular connection. The PPI polymer, poly(PPI), is successfully acquired by electropolymerization with the advantages of good stability, homogeneity and strong adherence toward the electrode surface. The as-prepared sensor exhibited brilliant electrochemical performance toward the multiplex detection of bases with significant peak separation, ensuring the possibility to distinguish four DNA bases without any separation pretreatment process. In this system, poly(PPI) displays three functions: (1) The enlarged π-conjugated architecture of poly(PPI) constructs a signal-enhancing system, which amplify the response current of the bases oxidation. (2) Non-planar growth of conducting polymer film could interact with the bases via π-π interactions, contributing to decreasing the activation energies of the electrocatalytic reactions and providing more recognition points for electrochemical sensing process. (3) The wire-like conducting skeleton of polymer can effectively improve the electrical conductivity and accelerate electron migration between the bases and electrode surface. To the best of our knowledge, no such works are reported on basis of PI derivatives without the assistance of extra-materials toward the detection of DNA bases. Our work provides a potential application of PI derivatives in biosensing fields as well as diseases diagnostics.

EXPERIMENTAL SECTIONS

Instruments and reagents. 9,10-phenanthraquinone, 4-bromonenzaldehyde, aniline, ammonium acetate and glacial acetic acid were purchased from Sigma-Aldrich Corporation (UAS). G, A, T, C and fish sperm DNA were acquired from Shanghai Macklin Biochemical Co., Ltd (China). A 0.1 M phosphate buffer solution (PBS) was obtained by mixing 0.2 M KH_2PO_4 and 0.2 M Na_2HPO_4. Bases solutions were made from dissolving them into 0.1 M NaOH. All reagents used in this experiment were of analytical grade without further purification process.

The ^1H NMR spectra was tested on a Bruker Avance 500 spectrometers at 400 MHz with tetramethylsilane (TMS) as an internal standard and deuterated dimethyl sulfoxide (DMSO) as a solvent. Scanning electron microscopy (SEM) images were performed on a Hitachi SU8020 scanning electron microscope (Japan). X-ray photoelectron spectroscopy (XPS) was performed on an ESCALAB-MKII 250 X-ray photoelectron spectrometer using Al Kα radiation. Fourier transform infrared (FTIR) spectra were measured on a Nicolet Impact 410 FTIR spectrometer.

All electrochemical experiments were conducted on a CHI 760E electrochemical workstation (CH instruments, Shanghai Chenhua Instrument Co., Ltd., China) in a three-electrode system, using the bare glassy carbon electrode (GCE) with 3 mm in diameter or modified GCE as working electrode, the platinum (Pt) wire as counter electrode and the saturated calomel electrode (SCE) as reference electrode. The square wave voltammetry (SWV) measurement was utilized for detecting bases and performed in 0.1 M PBS with initial potential at 0.4 V, finial potential at 1.8 V, amplitude of 25 mV and ΔE of 4 mV at 15 Hz.

Synthesis of the PPI monomer. The PPI monomer was prepared according to previous literature with a slight modification (Scheme S1 in the Supporting information).[32] Briefly, the mixture of 9,10-phenanthraquinone (1.0 g. 4.8 mmol), 4-bromobenzaldehyde (0.89 g, 4.8 mmol), aniline (24.0 mmol), ammonium acetate (19.2 mmol) and glacial acetic acid (72 mL) were refluxed under nitrogen atmosphere in a 120°C oil bath. After 4h, the mixture was cooled to room temperature and filtered. The obtained solid sample was washed with acetic acid/water (60 ml, 1:1, v:v) and water. Then, the solid product was dried under the vacuum to get the expected product with the yield > 80%.

Sensor fabrication. The fabrication and sensing procedure of the poly(PPI)/GCE is illustrated in Scheme 1. Prior to modification, the bare GCE was carefully polished with 0.3 and 0.05 μm Al_2O_3 powder on a polishing cloth to give a mirror surface and then washed with 1:1 nitric acid, ethanol and ultrapure water in an ultrasonic bath, respectively. The cleaned GCE was dried under a nitrogen steam. In order to get PPI modified electrode, the cleaned CGE was carried out in DMF/acetonitrile = 1:1 (v/v) solution containing 1.000 mg mL^{-1} PPI with 100.0 mM $LiClO_4$ as a supporting electrolyte through cyclic voltammetry by cyclic sweeping from – 1.8 to 1.8 V (vs Ag wire) at 0.1 V s^{-1} for 20 cycles. After electropolymerization, the modified electrode was washed with acetonitrile in order to remove the supporting electrolyte and monomers. Then, the poly(PPI)/GCE was obtained.

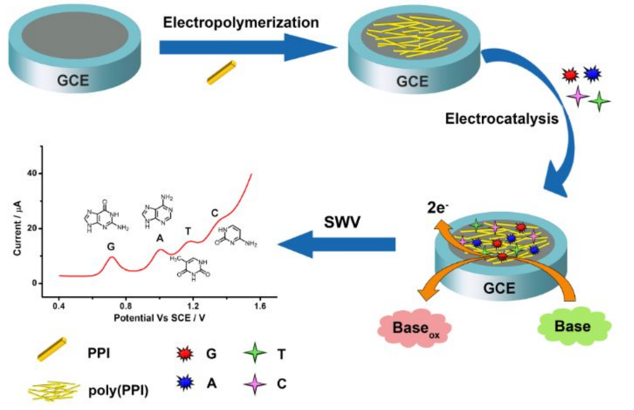

Scheme 1. The fabricating process of the poly(PPI)/GCE and DNA bases oxidation.

RESULTS AND DISCUSSIONS

Electropolymerization of PPI. The electrochemically deposition of the PPI film onto the cleaned GCE surface is displayed in Figure S1 in the Supporting information. An oxidation peak at about 1.1 V is observed, which can be attributed to the oxidation of tertiary amino and the formation of a radical cation $PPI^{\bullet +}$.[33] The second irreversible oxidation peak at around 1.6 V probably assigned to the oxidation of cation radical with undergoing a fast chemical reaction process (perhaps deprotonation).[34] The increase of peak current indicates that the conductive polymer film has formed at the surface of GCE. The electropolymerization mechanism of PPI was rarely reported from previous research. A hypothesis for structure of triphenylamine, which manifested the possibility of cation radical upon the formation of dimerization, was taken into consideration.[35,36] A pair of electron of tertiary amino in imidazole ring lost one electron to generate the radical cation. Then, the oxidative coupling occurs at the para-position of imidazole ring to form a dimeric. The possible electropolymerization pathway of PPI is exhibited in Figure S2 in the Supporting information.

Morphological and structural characterization. ^1H NMR spectra of PPI is displayed in Figure 1a. ^1H NMR (400 MHz, DMSO, 25°C, TMS, δ): 8.96 (d, J = 8.4 Hz, 1H, Ar H), 8.91 (d, J = 8.2 Hz, 1H, Ar H), 8.71 (d, J = 7.9 Hz, 1H, Ar H), 7.83–7.69 (m, 7H, Ar H), 7.63-7.56 (m, 3H, Ar H), 7.53 (d, J = 8.2 Hz, 2H, Ar H), 7.37 (t, J = 7.7 Hz, 1H, Ar H), 7.10 (d, J = 8.3 Hz, 1H, Ar H).[32]

As shown in Figure 1b, the FT-IR spectra of poly(PPI) is similar with that of the PPI with a little difference in the low frequency region 600-900 cm^{-1} of benzene ring substituents.[37] The signal of PPI at 1629 cm^{-1} is assigned to the C=C stretching vibration at the aromatic ring and the absorption band at 1393 cm^{-1} is attributed to the stretching vibration of tertiary amino group move to 1639 cm^{-1} and 1402 cm^{-1} in poly(PPI), respectively.[38] The monomer and its derived polymer show similar signals at 1271 cm^{-1} and 1272 cm^{-1} owing to the C-N stretching from tertiary amines.[39] The peaks at 1450 cm^{-1} of monomer and 1455 cm^{-1} of polymer are attributed to the C=N– stretching band of imidazole.[40] The absorption band at around 1050-1100 cm^{-1} region can be ascribed to the out of plane bending vibrations of aromatic ring. The peaks at the region from 690 to 550 cm^{-1} are assigned to the stretching vibrations of C-Br.[41] The peaks at 883 and 727 cm^{-1} disappear in the spectrum of poly(PPI), indicating the polymerization happened.

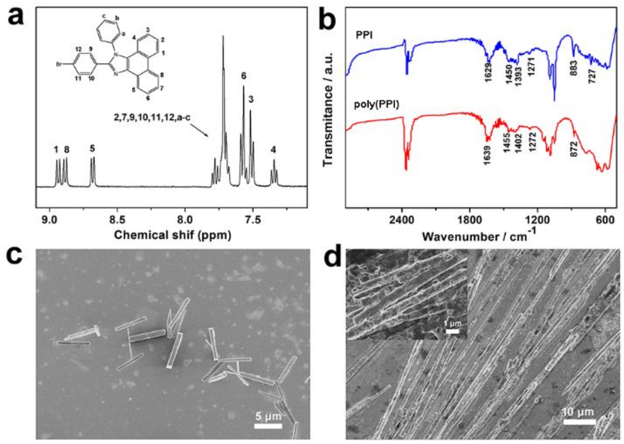

Figure 1. (a) ^1H NMR spectra of PPI, (b) FT-IR spectrum of PPI monomer and poly(PPI), SEM images of (c) PPI and (d) poly(PPI).

The characteristic band of poly(PPI) at ~872 cm^{-1} reveals the presence of 1,4-disubstituted phenyl ring in the polymerization procedure.[39] Hence, the proposed polymerization mechanism of PPI inferred from the FT-IR spectrum is consistent with our previous analysis. XPS spectrum was utilized to analyze the elemental compositions of the poly(PPI) (Figure S3). Along with the C 1s and N 1s, the XPS spectrum exhibits the signal of Br 3d at around 70 eV,[42] validating the existence of Br in poly(PPI).

The morphology of PPI and its polymer perform distinct difference in Figure 1c-d. The morphology of monomer displays a short rod-like texture with disordered distribution. After the electropolymerization of PPI, the polymer exhibits an order structure with nano-/microwire-like shape. Few studies explain the relevant morphologies of π-conjugated polymer. Based on the molecular wire theory,[18] we presume that the large-scale π-conjugation between the oligomer molecules makes the backbones growth with a linear structure under the steric effects, which gives birth to the "molecular wire". As we can see, much rougher surface can be found in the wire-like texture. The cross-link microwire-like texture could accelerate the electron transfer and provide larger active surface area, leading to higher electrocatalytic efficiency.

The electrochemical performance of the prepared electrode material was evaluated by CV technique. Figure S4a shows the CV curves recorded at bare GCE and poly(PPI)/GCE. The intensities of obtained redox peaks at bare GCE were low and the potential difference (ΔE_p) is determined to 173 mV. Compared to the bare GCE, the redox current responses of poly(PPI)/GCE are enhanced with a decreased ΔE_p of 141 mV, illustrating that the conducting polymer-based electrode perform the excellent conductivity. Furthermore, the electrochemical active surface area (A_e) of the electrodes were extracted with Randles-Sevcik equation:[43]

$$I_{pa} = (2.69 \times 10^5) A_e n^{3/2} D_0^{1/2} C_0 v^{1/2}$$

In which, n is the electron transfer number, D_0 represents the diffusion coefficient of $[Fe(CN)^6]^{4-}$ (6.3×10^{-6} cm^2 s^{-1}), C_0 represents the bulk concentration and v is the scan rate. The value of A_e at bare GCE and poly(PPI)/GCE are calculated to be 0.0857 and 0.1137 cm^2. The higher electroactive surface area of poly(PPI)/GCE could enhance the current response and benefit for improving the electrocatalytic activity.

The charge transfer property of electrode interface was probed by electrochemical impedance spectroscopy (EIS) (Figure S4b in the Supporting information). The Nyquist plots are composed of two portions, in which the semicircle part at higher frequencies is related with electron transfer-limited procedure and the linear portion at lower frequencies is attributed to the diffusion limited process. The charge transfer resistance (R_{ct}) equates the diameter of semicircle part in the EIS plot and can be inferred by fitting the data using relevant equivalent circuit (inset of Figure S4b) [44]. From the EIS profile, it is clear to observe that the semicircle diameter of GCE electrodeposited with poly(PPI) is much less than that of bare GCE. For bare GCE, the value of R_{ct} is estimated to be 306.9 Ω. After modified with poly(PPI), the R_{ct} value decreases rapidly to 98.23 Ω, confirming the superior electronic conductivity upon introducing the polymer film.

Electrochemical Characteristics of G, A, T and C at poly(PPI)/GCE. The redox characteristics of four DNA bases in 0.1 M PBS (pH 7.0) were investigated using CV methods at bare GCE and poly(PPI)/GCE in Figure 2a-d. Only a weak anodic peak is detected in bare GCE, indicating the poor redox property of bare electrode. Compared to the bare electrode, the poly(PPI)/GCE shows an increase of the current response and a decrease of the overpotential for the DNA bases, illustrating the superior electrochemical activity of poly(PPI) toward the bases oxidation. The observation of only an oxidation peak reveals that the redox procedures are chemically irreversible process. Meanwhile, the CV plots of poly(PPI)/GCE in the presence or absence of DNA bases are presented in Figure S5 in the Supporting information. No other peaks present in the blank scan, suggesting that the CV responses of poly(PPI)/GCE are absolutely from DNA bases oxidation. Furthermore, the SWV technique was utilized to investigate the possibility to detect the four bases. The electrochemical response of four bases were tested at bare GCE and poly(PPI)/GCE in Figure 2e. The SWV curve of bare GCE exhibits poor current response toward four

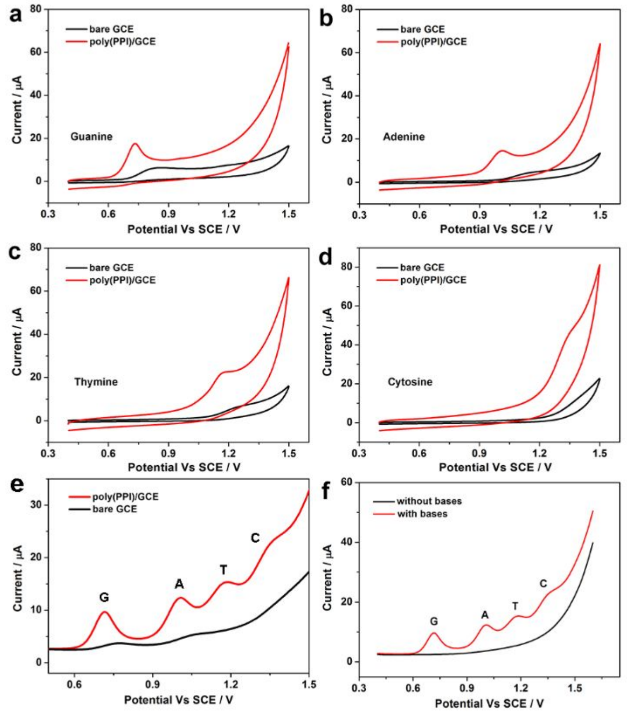

Figure 2. CV curves of (a) 100 μM G, (b) 100 μM A, (c) 300 μM T, (d) 300 μM C at bare GCE and poly(PPI)/GCE, (e) SWV plots of a mixture including 50 μM G, 50 μM A, 250 μM T, 250 μM C at bare GCE and poly(PPI)/GCE and (f) SWV plots of poly(PPI)/GCE in the presence and absence of 50 μM G, 50 μM A, 250 μM T, 250 μM C in 0.1 M PBS (pH 7.0).

bases. As expected, four apparent oxidation peaks can be distinguished on poly(PPI)/GCE at 0.714, 1.004, 1.177 and 1.353 V corresponding to G, A, T and C, respectively. The peak potential resolutions of bases are 290 mV for G and A, 173 mV for A and T, and 176 mV for T and C, displaying enough difference for their recognition and simultaneous determination in the mixture. The outstanding performance of poly(PPI)/GCE for DNA bases detection may be attributed as following aspects: (1) The extended π-conjugation of conjugated polymer may build a signal-amplification system, benefiting for collecting the minor current response. (2) The poly(PPI) film could have interaction with the bases via π-π interactions, which may contribute to diminishing the activation energies of the electrocatalytic reactions.[45] (3) The cross-link microwire-like skeleton can promote the electron transfer ability of the bases oxidation reactions.

Effect of pH on the oxidation current of DNA bases. The effect of pH toward DNA base determination was investigated via SWV method in different pH from 3.0 to 9.0 and the results are illustrated in Figure 3. As we can see, all the bases are detectable with poly(PPI)/GCE. Figure S6a displays the variation of oxidation peak current under different pH values. G and A perform the highest current responses at pH 3.0-4.0. The oxidation behavior of G and A could be related to the protonation. In acidic conditions, the electrochemical oxidation reaction of G and A became easier as a result of the existence of more protons, leading to the increase of the anodic peak currents.[46] Nevertheless, the weak current responses of T and C are exhibited in the pH 3.0 and 4.0, indicating the limited detection sensitivity at these pH conditions. Much higher current responses of T and C are observed at moderately alkaline conditions with the pH range from 8.0 to 9.0. Based on the research of pH condition optimization analysis, pH 7.0 is selected as the optimum pH value for the following study so as to mimic the physiological environment for the detecting biological samples.[47] The anodic peak potentials of DNA bases at different pH are recorded at Figure S6b in the Supporting information. The peak potentials move negatively with increasing the values of pH from 3.0 to 9.0, implying the existence of proton-transfer during the electrochemical oxidation of DNA bases. The peak potentials are proportional to pH values and the slopes acquired from G, A, T and C are 50.56 mV pH^{-1}, 57.85 mV pH^{-1}, 66.67 mV pH^{-1} and 51.54 mV pH^{-1}, respectively. The values approach the expected Nernstian theoretical value of 0.059 V pH^{-1}. The consequences confirm that the oxidation of DNA bases involve a two-electron/two-proton process in the rate-determining step.[48,49] The possible electrochemical oxidation mechanism of G, A, T and C were illustrated in Figure S7 in the Supporting information.[50]

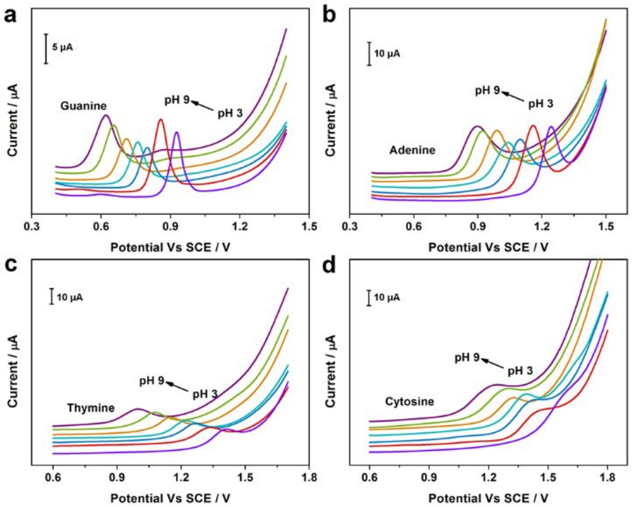

Figure 3. SWV curves of (a) 50 μM of guanine, (b) 100 μM of adenine, (c) 300 μM of thymine and (d) 300 μM of cytosine with different pH conditions from 3.0 to 9.0 at poly(PPI)/GCE in 0.1 M PBS.

Influence of scan rate on the oxidation of G, A, T and C. The effect of scan rate of poly(PPI)/GCE were recorded by linear sweep voltammetry (LSV) method (Figure S8 in the Supporting information). The oxidation currents of four bases are proportional to the scan rates. The corresponding linear regression equations of the currents and scan rates are expressed as follows:

$$\text{G:}\quad I\ (\mu\text{A}) = 0.1260v\ (\text{mV s}^{-1}) + 4.980 \quad (R^2 = 0.9902)$$

$$\text{A:}\quad I\ (\mu\text{A}) = 0.1436v\ (\text{mV s}^{-1}) + 5.340 \quad (R^2 = 0.9983)$$

$$\text{T:}\quad I\ (\mu\text{A}) = 0.1086v\ (\text{mV s}^{-1}) + 9.401 \quad (R^2 = 0.9953)$$

$$\text{C:}\quad I\ (\mu\text{A}) = 0.2621v\ (\text{mV s}^{-1}) + 21.02 \quad (R^2 = 0.9971)$$

The consequences demonstrated that the electrochemical oxidation reactions of G, A, T and C on poly(PPI)/GCE are surface-controlled process.[15] From previous reports, the accumulation time and potential could affect the oxidation of DNA bases. The details can be in the Supporting information in Figure S9-10. In this work, we detected the four bases without accumulation process in order to obtain efficient detection.

Individual and simultaneous electrochemical determination of G, A, T and C. The individual detections of purine and pyrimidine bases were recorded by SWV. As shown in Figure 4a, in presence of the A, the oxidation currents increase with the addition of G. The linear ranges of G at modified GCE are 3-50 μM and 50-300 μM. The linear regression equations are I (μA) = 0.1170c (μM) + 3.128 (R^2 = 0.9919) and I (μA) = 0.05703c (μM) + 6.059 (R^2 = 0.9942). Similarly, two linear regions are observed with increasing the concentration of A while keeping the concentration of G constant (Figure 4b). The linear ranges of A are from 1 to 50 μM and 50 to 300 μM. The respective linear regression equations are I (μA) = 0.1291c (μM) + 5.857 (R^2 = 0.9937) and I (μA) = 0.06214c (μM) + 9.203 (R^2 = 0.9925), respectively. It has been reported in earlier literatures that the linear calibration curves of G and A can be

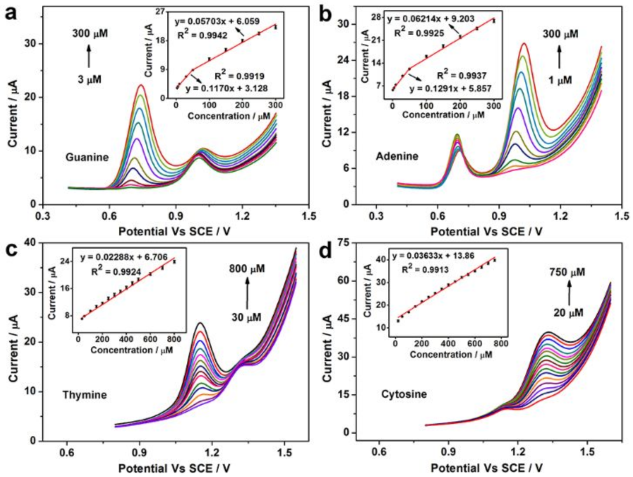

Figure 4. SWVs of various concentrations of (a) G in the presence of 30 μM A; (b) A in the presence of 50 μM G; (c) T in the presence of 100 μM C; and (d) C in the presence of 100 μM T, at poly(PPI)/GCE in 0.1 M PBS (pH 7.0).

Table 1. Comparison of different modified electrodes for simultaneous determination of DNA bases

Electrodes	Methods	DNA bases	Linear range (μM)	Detection limit (μM)	References
Au-rGO/MWCNTs/graphite	SWV	G	13-165	3.30	1
		A	15-185	3.70	
		T	47.6-800	7.90	
		C	54.0-900	9.00	
Cu@Ni/MWCNTs/GCE	DPV	G	1.0-180	0.17	52
		A	2.0-150	0.33	
Polyaniline/MnO_2/GCE	DPV	G	10-240	7.80	53
		A	10-150	7.70	
		T	10-1100	4.90	
		C	10-500	4.10	
β-Cyclodectrin/MWCNTs/GCE	DPV	G	100-280	0.033	54
		A	4.0-30	0.0007	
		T	80-400	0.006	
CuO NPsMCPE	DPV	G	1.0-94	0.687	55
		A	1.0-94	0.472	
		T	1.0-244	0.111	
MWCNT-Fe_2O_3@PDA-Ag/CPE	DPV	G	8.0-130	4.80	56
		A	10-120	2.90	
MoS_2-PCE	DPV	G	15-200	0.76	57
		A	12-120	2.38	
Poly(PPI)/GCE	SWV	G	3-300	0.28	This work
		A	1-300	0.24	
		T	30-800	3.2	
		C	20-750	6.8	

divided into two part regions. The first linear segment in relatively low concentrations can be attributed to an absorption process of purine at the electrode surface and the second linear segment at higher concentrations is associated with a diffusion procedure on the monolayer-covered surface.[51] As for T and C, the currents increase linearly with the concentration of T and G (Figure 4c-d). The regression equations of T and C are I (μA) = 0.02288c (μM) + 6.706 (R^2 = 0.9924) and I (μA) = 0.03633c (μM) + 13.86 (R^2 = 0.9913), respectively. The linear concentration regions are 30–800 μM for T and 20–750 μM for C. The detection limits with S/N of 3 are 0.28 μM, 0.24 μM, 3.2 μM and 6.8 μM for G, A, T and C, respectively.

It is clearly to observe that the oxidation peak potentials of four bases are obviously separated in Figure 2e, which indicates the possibility for simultaneous determination of the DNA bases. To evaluate the feasibility of the poly(PPI) modified sensor for the multiplex determination of G, A, T and C, the SWV of DNA bases in different concentrations was illustrated in Figure 5a. With the addition of the four bases, the current responses increase. A linear relationship exists between the concentrations of bases and electrochemical response. The concentration ranges for G, A, T and C are 5-90 μM, 5-90 μM, 30-320 μM, 30-320 μM, respectively. The regression equations of G, A, T and C are listed as follows:

G: I (μA) = 0.1063c (μM) + 4.413 (R^2 = 0.9909)

A: I (μA) = 0.1001c (μM) + 7.620 (R^2 = 0.9929)

T: I (μA) = 0.02937c (μM) + 8.292 (R^2 = 0.9889)

C: I (μA) = 0.04000c (μM) + 13.24 (R^2 = 0.9938)

Compared to the observation of individual detection, the determination linear ranges of four bases show some difference, which could be attributed to the existence of competitive adsorption of four bases at the active electrode surface. A list of detection toward four DNA bases with different modified electrodes is presented in Table 1, which are comparable to previous reported modified electrodes.

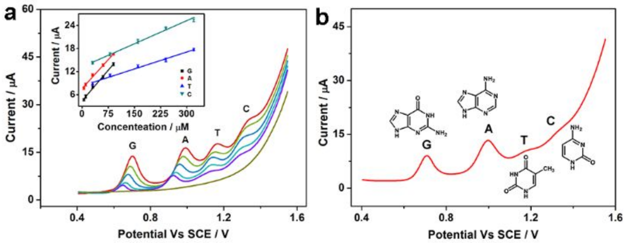

Figure 5. (a) SWV curves of simultaneous determination of mixture of G, A, T and C in 0.1 M PBS (pH 7.0). Inset: the calibration plots of currents versus concentrations. (b) SWV of fish sperm DNA sample in 0.1 M PBS (pH 7.0) on poly(PPI)/GCE.

Reproducibility, stability and interference studies in DNA bases analysis. The reproducibility of fabricated sensor was evaluated by ten successive measurements at same poly(PPI)/GCE (Figure S11 in the Supporting information). The results show the relative standard deviation (RSD) of 3.05%, 1.56 %, 2.05% and 0.779% for G, A, T and C, respectively, demonstrating the decent repeatability of the proposed sensor. To investigate the long-term stability of the sensor, the poly(PPI)/GCE was stored in air and utilized to detect four DNA bases for two or four weeks. The current responses remained 93.75%, 95.12%, 94.77% and 96.02% of the initial response of 30 μM G, 30 μM A, 200 μM T and 200 μM C after storage, indicating the good stability of present sensor.

The anti-interference ability toward the detection of bases was tested with the addition of foreign species in the mixture of bases (50 μM G, 50 μM A, 200 μM T and 200 μM C) in 0.1 M PBS (pH 7.0). The consequences reveal that 5.0 mM of Na^+, K^+, Ca^{2+}, Mg^{2+}, SO_4^{2-}, Br^- and 500 μM of L-proline, L-tyrosine, ascorbic acid, uric acid and glucose show no significant difference (signal change < 5%) for the detection of four bases (Table S1 in the Supporting information). The results confirm that the proposed sensor has highly selective and anti-interference capability which can be applied for the determination DNA bases in real samples.

Application for detecting bases in real sample. The practical application of modified electrode was assessed in fish sperm DNA system. Prior to analysis, 5 mg of fish sperm DNA was pretreated with 1.0 mL of 1.0 M HCl within a sealed 10 mL glass tube. After heating for 60 min at a boiling water bath, the solution was regulated to pH 7.0 using 1.0 mL of 1.0 M NaOH.[58] With addition of required amount of DNA sample, four anodic peaks of G, A, T and C was clearly presented on poly(PPI)/GCE (Figure 5b). The contents of G, A, T and C in acid-denatured fish sperm DNA can be determined from obtained linear regression equation and are calculated to be 22.18%, 27.04%, 28.16% and 22.62% (mol%), respectively. The ratio of (G + C)/(A + T) for fish sperm DNA sample is calculated as 0.81, which approach to the standard value of 0.77.[13]

CONCLUSION

In summary, an enlarged π-conjugated structure, PPI, was synthesized and exploited as an efficient electrode material for the determination of DNA bases for the first time. The poly(PPI) functionalized GCE performed excellent electric conductivity and remarkable electrocatalytic property toward the oxidation of four DNA bases by simple electropolymerization. The electrochemical sensor based on poly(PPI) realizes the individual and simultaneous detection of G, A, T and C with high sensitivity and selectivity. Moreover, the proposed sensor shows the advantages of extended linear region, satisfactory reproducibility and stability. The poly(PPI)/GCE has been successfully examined by detecting G, A, T and C in real samples with good accuracy, which show great promising in real time diagnostics. Compared to the previous researches, the present work shows a facile preparation process without using of extra-materials and present excellent electrocatalytic performance for distinguishing DNA bases. More importantly, our research not only presents a new sight to build a new kind of biosensor for DNA bases detection, but also can be easily extend to other PI derivatives to expand their application in electrochemical sensing system, biotechnological and medical diagnostics.

ASSOCIATED CONTENT

Supporting Information

The Supporting information is available free of charge on the ACS Publications website.

Electropolymeriation of PPI, XPS and electrochemical characterizations of poly(PPI), CVs of poly(PPI)/GCE, the effect of pH, scan rate, the effects of accumulation time and accumulation potential, reproducibility and selectivity of prepared sensor.

AUTHOR INFORMATION

Corresponding Authors

*Email: zzq@jlu.edu.cn

ORCID

Zhiquan Zhang：0000-0003-2764-321X

Author Contributions

The manuscript was written through contributions of all authors.

All authors have given approval to the final version of the manuscript.

Notes

The authors declare no competing financial interest.

ACKNOWLEDGMENTS

This work acknowledge support from Natural Science Foundation of Jilin Province (No. 2018010195JC).

REFERENCES

(1) Ng, K. L.; Khor, S. M. *Anal. Chem.* **2017**, *89*, 10004-10012.
(2) Vishnu, N.; Badhulika, S. *Biosens. Bioelectron.* **2019**, *124-125*, 122-128.
(3) Yang, T.; Chen, M.; Nan, F.; Chen, L.; Luo, X.; Jiao, K. *Journal of Materials Chemistry B* **2015**, *3*, 4884-4891.
(4) Cekan, P.; Sigurdsson, S. T. *J. Am. Chem. Soc.* **2009**, *131*, 18054-18056.
(5) Zhou, Y.; Yan, H.; Xie, Q.; Yao, S. *Talanta* **2015**, *134*, 354-359.
(6) Huang, Y.-F.; Chang, H.-T. *Anal. Chem.* **2007**, *79*, 4852-4859.
(7) Pang, S.; Zhang, Y.; Wu, C.; Feng, S. *Sensors and Actuators B: Chemical* **2016**, *222*, 857-863.
(8) Li, T.; Li, B.; Dong, S. *Analytical and Bioanalytical Chemistry* **2007**, *389*, 887-893.
(9) Yang, F.-Q.; Ge, L.; Yong, J. W. H.; Tan, S. N.; Li, S.-P. *J. Pharm. Biomed. Anal.* **2009**, *50*, 307-314.
(10) Sun, S.-W.; Liu, H.-L.; Zhou, Y.; Wang, F.-B.; Xia, X.-H. *Anal. Chem.* **2017**, *89*, 10858-10865.
(11) Anu Prathap, M. U.; Srivastava, R.; Satpati, B. *Electrochim. Acta* **2013**, *114*, 285-295.
(12) Ba, X.; Luo, L.; Ding, Y.; Zhang, Z.; Chu, Y.; Wang, B.; Ouyang, X. *Anal. Chim. Acta* **2012**, *752*, 94-100.
(13) Yari, A.; Derki, S. *Sensors and Actuators B: Chemical* **2016**, *227*, 456-466.
(14) Gao, S.; Li, H.; Li, M.; Li, C.; Qian, L.; Yang, B. *J. Solid State Electrochem.* **2018**, *22*, 3245-3254.
(15) Gao, Y.-S.; Xu, J.-K.; Lu, L.-M.; Wu, L.-P.; Zhang, K.-X.; Nie, T.; Zhu, X.-F.; Wu, Y. *Biosens. Bioelectron.* **2014**, *62*, 261-267.
(16) Liu, H.; Liu, C.; Gu, Y.; Li, C.; Yan, X.; Zhang, T.; Lu, N.; Zheng, B.; Li, Y.; Zhang, Z.; Yang, M. *Biosens. Bioelectron.* **2018**, *99*, 296-302.
(17) Mao, H.; Liang, J.; Zhang, H.; Pei, Q.; Liu, D.; Wu, S.; Zhang, Y.; Song, X.-M. *Biosens. Bioelectron.* **2015**, *70*, 289-298.
(18) Swager, T. M. *Acc. Chem. Res.* **1998**, *31*, 201-207.
(19) Gu, Y.; Yuan, R.; Yan, X.; Li, C.; Liu, W.; Chen, R.; Tang, L.; Zheng, B.; Li, Y.; Zhang, Z. *Anal. Chim. Acta* **2015**, *889*, 113-122.
(20) Yang, T.; Kong, Q.; Li, Q.; Wang, X.; Chen, L.; Jiao, K. *Polymer Chemistry* **2014**, *5*, 2214-2218.
(21) He, S.; He, P.; Zhang, X.; Zhang, X.; Li, C.; Dong, F.; Lei, H.; Liu, D. *J. Electroanal. Chem.* **2017**, *806*, 158-165.
(22) He, S.; He, P.; Zhang, X.; Zhang, X.; Liu, K.; Jia, L.; Dong, F. *Anal. Chim. Acta* **2018**, *1031*, 75-82.
(23) Liu, H.; Wang, G.; Chen, D.; Zhang, W.; Li, C.; Fang, B. *Sensors and Actuators B: Chemical* **2008**, *128*, 414-421.
(24) Steck, E. A.; Day, A. R. *J. Am. Chem. Soc.* **1943**, *65*, 452-456.
(25) Zhang, L.-K.; Wu, G.-F.; Zhang, Y.; Tian, Y.-C.; Tong, Q.-X.; Li, D. *RSC Advances* **2013**, *3*, 21409-21412.
(26) Subeesh, M. S.; Shanmugasundaram, K.; Sunesh, C. D.; Won, Y. S.; Choe, Y. *Journal of Materials Chemistry C* **2015**, *3*, 4683-4687.
(27) Liao, S.; Zhang, Z.; Wu, Q.; Wang, X.; Mei, W. *Biorg. Med. Chem.* **2014**, *22*, 6503-6508.
(28) Wang, S.; Li, H.; Chen, C.; Zhang, J.; Li, S.; Qin, X.; Li, X.; Wang,

K. *Bioorg. Med. Chem. Lett.* **2012**, *22*, 6347-6351.

(29) Jędrzejewska, B.; Gordel, M.; Szeremeta, J.; Grela, I.; Samoć, M. *Dyes and Pigments* **2017**, *136*, 150-160.

(30) Chen, W.-C.; Yuan, Y.; Xiong, Y.; Rogach, A. L.; Tong, Q.-X.; Lee, C.-S. *ACS applied materials & interfaces* **2017**, *9*, 26268-26278.

(31) Chen, W. C.; Yuan, Y.; Wu, G. F.; Wei, H. X.; Tang, L.; Tong, Q. X.; Wong, F. L.; Lee, C. S. *Advanced Optical Materials* **2014**, *2*, 626-631.

(32) Li, W.; Liu, D.; Shen, F.; Ma, D.; Wang, Z.; Feng, T.; Xu, Y.; Yang, B.; Ma, Y. *Adv. Funct. Mater.* **2012**, *22*, 2797-2803.

(33) Ashok Kumar, S.; Chen, S. L.; Chen, S. M. *Electroanalysis: An International Journal Devoted to Fundamental and Practical Aspects of Electroanalysis* **2009**, *21*, 1379-1386.

(34) Francke, R.; Little, R. D. *J. Am. Chem. Soc.* **2013**, *136*, 427-435.

(35) Yen, H.-J.; Liou, G.-S. *Org. Electron.* **2010**, *11*, 299-310.

(36) Santra, D. C.; Nad, S.; Malik, S. *J. Electroanal. Chem.* **2018**, *823*, 203-212.

(37) Hsiao, S.-H.; Lu, H.-Y. *Polymers* **2017**, *9*, 708.

(38) Xiao, X.; Zhou, B.; Tan, L.; Tang, H.; Zhang, Y.; Xie, Q.; Yao, S. *Electrochim. Acta* **2011**, *56*, 10055-10063.

(39) Kvarnström, C.; Petr, A.; Damlin, P.; Lindfors, T.; Ivaska, A.; Dunsch, L. *J. Solid State Electrochem.* **2002**, *6*, 505-512.

(40) Raj, V.; Madheswari, D.; Mubarak Ali, M. *J. Appl. Polym. Sci.* **2012**, *124*, 1649-1658.

(41) Popov, A. A.; Senyavin, V. M.; Granovsky, A. A. *Chem. Phys. Lett.* **2004**, *383*, 149-155.

(42) Xu, J.; Jeon, I. Y.; Seo, J. M.; Dou, S.; Dai, L.; Baek, J. B. *Adv. Mater.* **2014**, *26*, 7317-7323.

(43) Li, C.; Wu, R.; Zou, J.; Zhang, T.; Zhang, S.; Zhang, Z.; Hu, X.; Yan, Y.; Ling, X. *Biosens. Bioelectron.* **2018**, *116*, 81-88.

(44) Guo, X.; Kulkarni, A.; Doepke, A.; Halsall, H. B.; Iyer, S.; Heineman, W. R. *Anal. Chem.* **2011**, *84*, 241-246.

(45) Arvand, M.; Ardaki, M. S. *Anal. Chim. Acta* **2017**, *986*, 25-41.

(46) Qin, X.; Liu, X.; Hong-bo, L.; Li-na, Y.; Xiaoya, H. *Biosens. Bioelectron.* **2013**, *42*, 355-361.

(47) Ferancová, A.; Rengaraj, S.; Kim, Y.; Labuda, J.; Sillanpää, M. *Biosens. Bioelectron.* **2010**, *26*, 314-320.

(48) Wang, D.; Huang, B.; Liu, J.; Guo, X.; Abudukeyoumu, G.; Zhang, Y.; Ye, B.-C.; Li, Y. *Biosens. Bioelectron.* **2018**, *102*, 389-395.

(49) Kaur, B.; Srivastava, R. *Electrochim. Acta* **2014**, *133*, 428-439.

(50) Ouyang, X.; Luo, L.; Ding, Y.; Liu, B.; Xu, D. *J. Electroanal. Chem.* **2014**, *735*, 51-56.

(51) Fan, Y.; Huang, K.-J.; Niu, D.-J.; Yang, C.-P.; Jing, Q.-S. *Electrochim. Acta* **2011**, *56*, 4685-4690.

(52) Wang, D.; Huang, B.; Liu, J.; Guo, X.; Abudukeyoumu, G.; Zhang, Y.; Ye, B.-C.; Li, Y. *Biosens. Bioelectron.* **2018**, *102*, 389-395.

(53) Prathap, M. A.; Srivastava, R.; Satpati, B. *Electrochim. Acta* **2013**, *114*, 285-295.

(54) Shen, Q.; Wang, X. *J. Electroanal. Chem.* **2009**, *632*, 149-153.

(55) Ks, S.; B, M.; N, K. S. *Sensors and Actuators A: Physical* **2018**, *280*, 277-286.

(56) Yari, A.; Derki, S. *Sensors and Actuators B: Chemical* **2016**, *227*, 456-466.

(57) Vishnu, N.; Badhulika, S. *Biosens. Bioelectron.* **2019**, *124*, 122-128.

(58) Deng, C.; Xia, Y.; Xiao, C.; Nie, Z.; Yang, M.; Si, S. *Biosens. Bioelectron.* **2012**, *31*, 469-474.

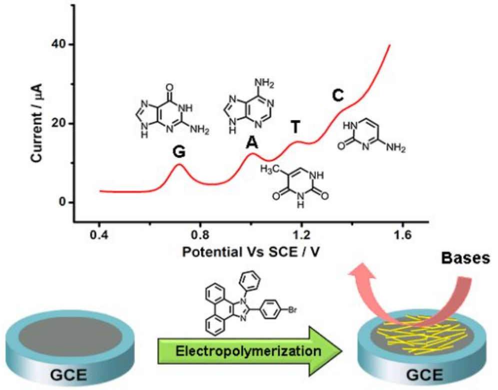

Table of Contents